Int. J. Heat Mass Transfer. Vol. 28, No. 2, pp. 383–394, 1985
Printed in Great Britain

0017–9310/85 $3.00 + 0.00

Solid conduction in low d_t/d_p beds of spheres, pellets and rings

MARIA M. MELANSON and ANTHONY G. DIXON
Department of Chemical Engineering, Worcester Polytechnic Institute, Worcester, MA 01609, U.S.A.

(*Received* 6 *March* 1984 *and in revised form* 2 *July* 1984)

Abstract—Experimental measurements of effective thermal conductivity and wall heat transfer coefficients were made for stagnant annular fixed beds of low tube-to-particle diameter ratio. A wide range of particle shapes, sizes and thermal conductivity was covered.

Empirical correlations are given for the wall-to-solid heat transfer coefficient, which becomes important for low d_t/d_p. Predictive formulas for thermal conductivity were tested, and recommendations made on their use. Both parameters were found to be relatively insensitive to particle shape.

The results are applied to the estimation of effective conductivity in the cylindrical beds of industrial practice.

INTRODUCTION

THE CYLINDRICAL packed bed is probably the most popular form of chemical reactor in use today, due largely to its ability to achieve high throughput, its relative freedom from mechanical problems, and the availability of much accumulated design and operational knowledge. One particularly important area of use is to carry out highly-exothermic catalytic reactions, for example *o*-xylene oxidation to phthalic anhydride or the production of ethylene oxide from ethylene. It is vitally important to prevent temperature excursions in such reactors as they may lead to poor selectivity for cases in which competing reactions occur, or to rapid deactivation of an expensive catalyst. In such cases the reactor takes the form of a bundle of long narrow tubes surrounded by a heat exchange medium, usually a liquid coolant. The tubes may be many hundreds of particle diameters long, but only a few diameters across, thus facilitating heat loss radially through the walls of the tube. For these reasons attention has been focused in recent years on the modelling of radial heat transfer in fixed beds of low tube-to-particle diameter ratio [1–5].

The use of continuum models is common in fixed bed heat transfer work. These may be pseudohomogeneous, in which case the bed is modelled as a single phase with effective axial and radial conductivities superimposed upon a bulk flow, or heterogeneous, for which both solid and fluid are envisioned as forming continua, coexisting at every point of the bed. Such an approach can be justified when the discrete particles are small compared to the macroscopic gradients in the bed, if necessary by invoking an averaging technique. For large particles it is difficult to rigorously show the validity of continuum models, however, two powerful reasons for retaining them are their mathematical tractibility and the lack of any convincing alternative. It has been shown that a two-dimensional pseudohomogeneous model can indeed represent radial and axial temperature profiles in a low d_t/d_p bed [2]. The price that must be paid is that the effective parameters must be correlated against the ratio d_t/d_p. This is also true for heterogeneous continuum model parameters.

For fixed beds of high d_t/d_p ratio the extra resistance to heat transfer in the near-wall region, caused by the ordering of the packing by the wall, is idealized to be a resistance at the wall, represented by the apparent wall heat transfer coefficient h_w (or h_{wf} and h_{ws} in each phase of a heterogeneous model). The effective radial conductivity k_r is then associated with the bed center and is assumed constant (and similarly for k_{rs} and k_{rf}). For $d_t/d_p < 10$ wall effects are present across the whole bed and there is no true bed center. Thus k_r may not be free of wall effects; however, it is expedient to continue to employ k_r and h_w, until fixed bed structure is understood well enough to predict the radial variation of k_r.

In this work, conductivities used in a model jointly with wall heat transfer coefficients will be referred to as 'bed-center' values, as opposed to 'bed-average' conductivities, which include all wall effects. For large d_t/d_p there is little or no difference between the two types; for small d_t/d_p the extra wall resistance in the fluid phase has been previously investigated [5]. For the solid phase the possibility of extra wall resistance and of significant differences between k_{rs} and $\bar{k}_{rs}$ has not been adequately pursued.

The objectives of this work are to investigate the importance of the wall-to-solid heat transfer coefficient h_{ws}, to relate the two solid phase conductivities k_{rs} and $\bar{k}_{rs}$, and to evaluate existing theoretical formulas for prediction of these quantities. Particular attention will be paid to the low d_t/d_p case, and to the ability of the formulas to handle different packing shapes, such as spheres, pellets and hollow pellets (rings), which are common catalytic supports.

NOMENCLATURE

a inner bed radius [m]
b outer bed radius [m]
d_p pellet diameter [m]
d_{pv} equivalent pellet diameter [m]
d_t tube diameter [m]
d_E annular diameter, $2(b-a)$ [m]
G superficial mass flow rate [kg/m^2 s]
h apparent interphase heat transfer coefficient [w/m^2 °C]
h_w apparent wall heat transfer coefficient [w/m^2 °C]
h_w° stagnant bed wall heat transfer coefficient [w/m^2 °C]
h_{wa} apparent inner wall heat transfer coefficient [w/m^2 °C]
h_{wb} apparent outer wall heat transfer coefficient [w/m^2 °C]
h_{wf} wall–fluid heat transfer coefficient [w/m^2 °C]
h_{ws} wall–solid heat transfer coefficient [w/m^2 °C]
h_{rv} fluid-phase radiative heat transfer coefficient [w/m^2 °C]
h_{rs} solid-phase radiative heat transfer coefficient [w/m^2 °C]
h_{fs} fluid–solid heat transfer coefficient [w/m^2 °C]
k_r radial effective conductivity [w/m°C]
k_r° stagnant bed radial effective conductivity [w/m°C]
$\bar{k}_r^\circ$ average stagnant bed radial effective conductivity [w/m°C]
k_{rf} radial conductivity of fluid phase [w/m°C]
k_{rs} radial conductivity of solid phase [w/m°C]
$\bar{k}_{rs}$ average radial conductivity of solid phase [w/m°C]
k_f molecular conductivity of fluid [w/m°C]
k_p pellet conductivity [w/m°C]
k_R radiation conductivity [w/m°C]
l_v effective pellet thickness [m]
Q_R radial heat flow [kJ/s]
R tube radius [m]
r radial coordinate [m]
T bed temperature, one-phase model [°C]
T_{wa} temperature of inner annular wall [°C]
T_{wb} temperature of outer annular wall [°C]
U overall heat transfer coefficient [w/m^2 °C].

Dimensionless parameters

Bi_a apparent inner wall Biot number, $h_{wa}a/k_r$
Bi_b apparent outer wall Biot number, $h_{wb}b/k_r$
Bi_f fluid–wall Biot number, $h_{wf}R/k_{rf}$
Bi_s solid–wall Biot number, $h_{ws}R/k_{rs}$
e emissivity
N_S interphase heat transfer group, aR^2h/k_{rs}
Nu_{fs} fluid–solid Nusselt number, $h_{fs}d_p/k_f$
Pe_r effective radial Peclet number, Gc_pd_p/k_r
Pe_{rf} radial fluid Peclet number, Gc_pd_p/k_{rf}
Pr Prandtl number, $\mu c_p/k_f$
Re Reynolds number, Gd_p/μ
y normalized radial coordinate (r/R or r/b).

Greek symbols

ε bed voidage
ϕ dimensionless pellet thickness (l_v/d_p)
κ conductivity ratio (k_p/k_f).

All heat transfer parameters defined in terms of total area (void and nonvoid) normal to the direction of heat transfer.

LITERATURE REVIEW

There have been many investigations, both theoretical and experimental, intended to determine the effective solid phase conductivity k_{rs}, in a fixed bed. In spite of these efforts, this parameter cannot yet be predicted accurately.

Early experimental investigations, such as [6], carried out transient heating of a cylindrical stagnant bed. More recently, two steady-state techniques have replaced this method. The first is to estimate values of effective radial conductivity k_r from experiments with flowing fluids. These are plotted against Re and a fitted straight line is extrapolated to stagnant conditions, $Re = 0$, where the intercept gives k_r°, which for a gaseous fluid phase differs only slightly from k_{rs}. Recent work [2, 5] has shown that at lower Re there is interaction between fluid and solid phase contributions to k_r, so that the data do not extrapolate linearly to $Re = 0$ except at extremely high d_t/d_p values.

A more reliable method is to make experimental measurements in an annular bed, so that a temperature difference may be maintained in the bed even with a stagnant fluid [7–10]. It is important in such work to eliminate wall effects if the solid phase conductivity obtained is to be truly that of the bed center. Most data reported in the literature by this method are in fact the bed-average values $\bar{k}_{rs}$ which include resistance at the walls. A correction factor for these values has been

proposed by Wellauer *et al.* [4] in the form

$$k_{rs} = \bar{k}_{rs}\left\{1 + 2.66\sqrt{\frac{d_p}{d_t}}\right\} \quad (1)$$

which the authors also used to obtain k_{rs} for cylindrical beds.

The effect of this formula is rather large; for $d_t/d_p = 8.0$, the value of k_{rs} is over twice that of $\bar{k}_{rs}$. Use of this formula for small d_t/d_p would change predictions of effective parameters quite considerably. As the formula is based on relatively few data from annular beds, together with the assumption that the inner and outer wall Biot numbers are equal, it requires further work to justify its use for cylindrical beds.

Several theoretical formulas have been proposed with the object of predicting k_r° (or equivalently k_{rs}) *a priori*, from a knowledge of only the true pellet conductivity k_p, the fluid phase conductivity k_f and the bed voidage ε. In a recent study, Crane and Vachon [11] have presented an illuminating classification of the theoretical models, which forms an appropriate basis for this review.

The first group is the *Fourier's law models* [12–17], in which an ideal geometry is assumed, giving rise to differential equations which can be solved analytically for the temperature field. The effective conductivity is then obtained from Fourier's law, and must somehow be related to the true packing state found in random fixed beds. Many of these models have been developed in the study of diffusion or conduction in periodic media [15, 16], and the various approaches to the solution of the governing equations have been reviewed and unified by Chang [17]. The work of Balakrishnan and Pei [14], which was undertaken principally to cast light upon the overall bed heat transfer coefficient, included solid-to-fluid convective heat transfer, which led to distorted isotherms within the spherical packing. The conductivity obtained from such a temperature field does not represent solid-phase conduction alone, but also a convective effect.

The Fourier's law approach is mathematically rigorous, however, it is very far from being able to allow for different particle shapes, or for wall effects, both of which are important in applications. There may be some hope that regular geometries can be representative of random packing, according to Chang [17], but at present it is necessary to turn to simpler and more flexible methods.

The second group of models is termed *Ohm's law models* [18–24]; in these, one-dimensional heat transfer is assumed to occur through simplified, repetitive geometries, allowing the development of a thermal resistance network, which is then solved for the total resistance and thus the effective conductivity. This category can be further divided into two subcategories: (i) zero lateral conductivity (i.e., zero heat flux normal to the main heat transfer direction), so that the heat flux remains constant in the transfer direction; and (ii) infinite lateral conductivity, so that the isotherms are parallel and normal to the heat flow direction. Each of these subgroups gives a different resistance network for a specified geometry. Crane and Vachon [11] developed models for each of (i) and (ii), and found that the predictions formed lower and upper bounds respectively to a large amount of experimental data on k_r°.

Probably the best known zero lateral conductivity Ohm's law model is that developed for spheres by Kunii and coworkers [18–20], which includes conduction and radiation through the fluid, solid-to-solid radiation, conduction through finite area contacts and a series mechanism for conduction through stagnant fillets near the contact points. The chief assumption of the model is that the thermal resistance of the fillets may be represented by an equivalent film thickness l_v, which can be related to the packing state through the bed voidage ε. The l_v can be found for two regular packings, cubic open-packed and hexagonal close-packed, and linear interpolation is used to obtain l_v for packings of intermediate void fraction. The model should therefore be treated with caution for nonspheres or for voidages outside a limited range ($0.260 < \varepsilon < 0.476$). Kunii and Smith [19] showed that agreement to within $\pm 30\%$ for stagnant fluid experiments could be found, but comparison with extrapolation results for flowing fluids was not so good. Similar observations led Specchia *et al.* [21] to attempt a purely empirical modification of the Kunii–Smith formula to fit extrapolated values, an approach which cannot be recommended for low d_t/d_p beds.

Wishing to have a formula that was usable for the entire voidage range, Zehner and Schlünder [22] employed a variable particle shape in their cell model, to try to remedy the problems of sphere-based formulas. To account for bed geometry and the line and area contacts possible with nonspherical packings, they found it necessary to introduce a form factor C which was fitted to experimental data and depended only on packing type. Agreement with a mixture of data was obtained to within $\pm 30\%$ again. The Zehner–Schlünder model was later extended by Bauer and Schlünder [23], to allow for shape effects in more detail, nonmonodisperse packings, surface oxidation of metallic packings, radiation and low-pressure effects. The last two had previously been considered by the original authors [24].

The contribution of radiation to solid conductivity increases with temperature, and has been specifically treated by several authors [12, 25, 26], in addition to being included in the above formulas. Some mechanisms for conduction in beds of spheres are important only for very low pressures, such as conduction through a finite contact area [27] and the temperature jump, or Smoluchowski, effect [28]. These latter are not considered further in this work.

Comparisons of their own formulas to experimental data have been made by several authors [11, 19, 22, 23, 29], but there has been little or no attempt to discriminate between the available models. These

comparisons are difficult to evaluate as the data used are usually a mixture of results from both flowing fluid and annular bed experiments. In addition, many workers do not report values of k_p or d_t/d_p, especially in earlier studies. On the basis of the above review, the models of Kunii and Smith [19] and Bauer and Schlünder [23], are selected for further testing against the low d_t/d_p data for various packing shapes obtained in the present work.

In contrast, there is very little information available for the stagnant wall heat transfer coefficient, h_w°, or the solid phase contribution h_{ws}. Some values are available for the inner wall of an annular bed [8], and Paterson [10] obtained very limited data for both wall Biot numbers. The most extensive study was that of Ofuchi and Kunii [30], however they used a bed with slab geometry, and thus plane walls. For low d_t/d_p, the curvature of the wall will certainly influence the results. Ofuchi and Kunii [30] also provides a predictive formula for h_{ws}, based on a modified version of the Kunii–Smith formula. A formula based on the addition of radiation, gas-phase conduction and point contact mechanisms has been proposed by Schlünder [31, 32], and finally Olbrich [33] has theoretically derived a lower bound for Bi_s. These models will also be tested against data from this study.

EXPERIMENTAL

An apparatus similar to that of Yagi and Kunii [8] was used in this study. Steady-state heat flow was measured in an annular bed where the walls were maintained at different temperatures. A schematic of the experimental apparatus is shown in Fig. 1. The annular bed consisted of a steam jacket which served as the outer wall (75 mm i.d.) and a centered water pipe (10.4 mm o.d.) which acted as the inner wall. The total length of the column was 465 mm. A steam trap was placed in line before the entrance to the steam jacket in order to remove condensate from the steam supply. A drain was located at the base of the column for the removal and collection of the jacket condensate. The water flowrate was adjusted in order that the temperature rise was always less than 0.5°C, ensuring a uniform temperature along the inner wall for its entire length. Uniform wall temperatures at the inner and outer walls of the column permitted the assumption of a purely radial heat flux in the middle portion of the bed, where end effects could be neglected.

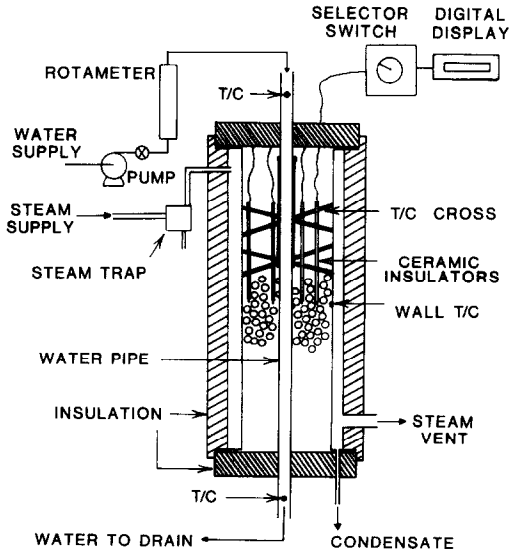

FIG. 1. Schematic of experimental apparatus.

The radial bed temperature profiles, wall temperatures, and water temperatures were measured using 30 gauge chromel–alumel, fiberglass-sheathed thermocouples. Temperature measurements were made at six radial positions; one at each wall and four in the bed itself. The four bed temperatures were measured by thermocouples fixed in a four-arm cross similar to that of Paterson [10], which was buried within the bed to eliminate end effects. The thermocouples were held rigid by 3.175 mm o.d. ceramic insulators which extended 90 mm below the lower arms of the cross. Temperature measurements were made at a depth of approximately 200 mm. The radial positions of the thermocouples were 5.2, 11.4, 17.0, 24.2, 31.7, and 37.5 mm from the bed center.

Many types of packing were used in this study. These packings included a variety of shapes, sizes, and materials. Spheres, solid cylinders, thin-walled hollow cylinders, and thick-walled hollow cylinders were employed. A description of the packings investigated appears in Table 1; the values of k_p were estimated, and the bed average void fractions for each packing were obtained experimentally by water displacement.

Two experiments were performed with each packing material, so that the effects of repacking on the temperature profile and heat flux could be taken into consideration. Each experiment was divided into two parts for analysis; a blank run without water flow used to determine the heat loss from the column, and a test run with water flow. For each run, the system was allowed to come to steady state, then several samples of condensate were taken, each over a 20 minute interval. This procedure was performed to check the consistency of the inlet steam quality. The condensate samples were collected in an ice-bath-cooled receptacle, minimizing the evaporation during the 20 minute interval. Temperature profiles and condensate sample weight were recorded; some typical profiles are shown in Fig. 2.

The analysis of the data followed closely the procedure given by Yagi and Kunii [8]. The energy balance differential equation may be solved to give

$$T = A \ln y + B \tag{2}$$

where

$$A = \frac{T_{wb} - T_{wa}}{\ln\left(\frac{b}{a}\right) + \frac{1}{Bi_b} + \frac{1}{Bi_a}} \tag{3}$$

Table 1. Details of packings and experimental results

Packing	Symbol	d_{pv} (mm)	$k_p\left(\frac{w}{mK}\right)$	ε	$\bar{k}_r\left(\frac{w}{mK}\right)$	$k_r^\circ\left(\frac{w}{mK}\right)$	Bi_a	Bi_b
6.35 mm nylon spheres	○	6.35	0.242	0.392	0.175	0.214	2.69	14.20
7.938 mm nylon spheres	○	7.938	0.242	0.402	0.155	0.209	1.77	7.76
9.525 mm nylon spheres	○	9.525	0.242	0.422	0.164	0.240	1.39	5.35
12.70 mm nylon spheres	○	12.70	0.242	0.433	0.158	0.279	0.833	3.52
25.40 mm nylon spheres	○	25.40	0.242	0.511	0.110	0.253	0.427	5.08
19.05 mm polystyrene spheres	⊖	19.05	—	0.506	0.108	0.194	0.803	3.26
6.35 mm steel spheres	●	6.35	63.18	0.392	0.495	0.550	4.48	∞
9.525 mm steel spheres	●	9.525	63.18	0.422	0.468	0.791	0.924	5.78
12.70 mm steel spheres	●	12.70	63.18	0.433	0.424	0.716	0.817	7.37
6.35 × 6.35 mm Al cylinders	■	7.268	152	0.380	1.026	1.480	2.46	∞
9.525 × 9.525 mm Al cylinders	■	10.901	152	0.418	0.474	1.158	0.365	11.02
12.70 × 12.70 mm Al cylinders	■	14.535	152	0.436	0.286	0.925	0.296	2.60
9.525 × 9.525 × 4.673 mm Al hollow cylinders	◧	10.901	152	0.531	0.403	1.161	0.275	8.65
12.70 × 12.70 × 6.35 mm Al hollow cylinders	◧	14.535	152	0.545	0.375	1.365	0.215	1.87
6 × 6 × 4 mm glass hollow cylinders	▥	6.867	1.23	0.612	0.232	0.303	1.88	14.07
8 × 8 × 6 mm glass hollow cylinders	▥	9.156	1.23	0.705	0.189	0.280	1.23	7.03
9.525 mm porous ceramic spheres	⊘	9.525	1.18	0.468	0.180	0.313	0.778	6.646
12.70 mm porous ceramic spheres	⊘	12.70	1.18	0.463	0.196	0.452	0.464	2.477
9.525 mm porous ceramic cylinders	▨	10.901	1.18	0.406	0.214	0.390	0.706	5.256
7.94 × 7.94 × 3.97 mm ceramic hollow cylinders	▥	9.085	1.18	0.439	0.294	0.489	0.846	7.801
13 × 13 × 7 mm ceramic hollow cylinders	▥	14.879	—	0.638	0.196	0.469	0.437	2.343

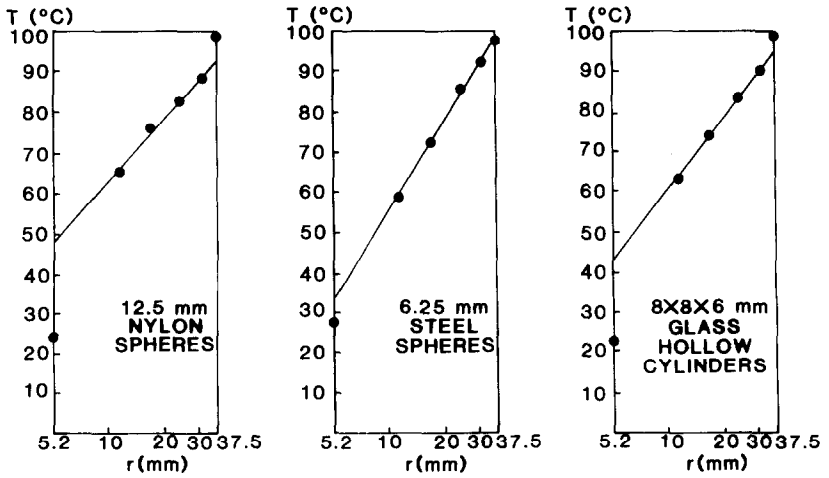

FIG. 2. Typical radial temperature profiles.

and

$$B = T_{wb} - A\frac{1}{Bi_b}. \quad (4)$$

The condensate per unit time is given by

$$Q_R = -(2\pi L)k_r^\circ \left.\frac{\partial T}{\partial y}\right|_{y=1} \quad (5)$$

where Q_R has been adjusted for heat losses using the blank run results, as detailed in [8]. The above equations employ k_r° and both wall heat transfer coefficients; the equations for bed-average $\bar{k}_r^\circ$ may be obtained simply by letting Bi_a, Bi_b tend to infinity in equations (3) and (4), and replacing k_r° by $\bar{k}_r^\circ$ in equation (5).

According to equation (2), T should plot linearly with ln y, and this was true of all runs, confirming the assumption of purely radial heat flow in the bed center. A criterion given by Koya and Kunii [9] was used to justify neglect of natural convection.

A least squares fit of the bed interior temperatures gave the slope A and intercept B of equation (2), then Bi_a and Bi_b were found from wall temperatures and equations (3) and (4). The heat flux and equation (5) then yielded k_r° or $\bar{k}_r^\circ$, according to model.

Results for the bed average effective thermal conductivity, bed center effective thermal conductivity, and wall heat transfer coefficients are shown in Table 1 for each packing. Inner and outer wall Biot numbers were also calculated and tabulated. The symbol key for Figs. 3–7 is presented in this table; note that symbol shapes reflect particle shapes, and thermal conductivity (high or low) is indicated by shading.

PREDICTION FORMULAS FOR SOLID THERMAL CONDUCTIVITY

Two of the most popular formulas for k_r° are compared to the data in this section.

Formula of Kunii and Smith [19]

Omitting the finite area contact term this formula becomes

$$\frac{k_r^\circ}{k_f} = \varepsilon\left[1 + \frac{h_{rv}d_p}{k_f}\right] + \left[\frac{(1-\varepsilon)}{\dfrac{1}{d_p/l_v + d_p h_{rs}/k_f} + \dfrac{2}{3\kappa}}\right] \quad (6)$$

with

$$h_{rs} = 2.27\times10^{-7}\frac{e}{2-e}T^3 \quad \text{w/m}^2\,\text{K} \quad (7)$$

$$h_{rv} = 2.27\times10^{-7}\left[1 + \frac{\varepsilon}{2(1-\varepsilon)}\frac{1-e}{e}\right]^{-1}T^3 \quad \text{w/m}^2\,\text{K} \quad (8)$$

and

$$\phi = \frac{l_v}{d_p} = \begin{cases}\phi_2 & \varepsilon < 0.26\\ \phi_2 + (\phi_1 - \phi_2)\dfrac{\varepsilon - 0.26}{0.476 - 0.26} & 0.26 < \varepsilon < 0.476\\ \phi_1 & \varepsilon > 0.476\end{cases} \quad (9)$$

where

$$\phi_1 = \frac{0.333\left(1-\frac{1}{\kappa}\right)^2}{\ln\{\kappa - 0.577(\kappa-1)\} - 0.423\left(1-\frac{1}{\kappa}\right)} - \frac{2}{3\kappa} \quad (10)$$

$$\phi_2 = \frac{0.072\left(1-\frac{1}{\kappa}\right)^2}{\ln\{\kappa - 0.925(\kappa-1)\} - 0.075\left(1-\frac{1}{\kappa}\right)} - \frac{2}{3\kappa}. \quad (11)$$

As ε is being used as an indicator of packing state, a local value would give a local state and thus a local k_r°, whereas a bed average ε would give $\bar{k}_r^\circ$, the bed average stagnant conductivity. The bed average ε is all that is available, therefore the appropriate comparison is with the $\bar{k}_r^\circ$, and this is shown in Fig. 3.

The only adjustment to the formula for nonspherical particles was to use the diameter of the equivalent-volume sphere (neglecting hollow spaces) d_{pv} in place of d_p in equation (6). In spite of this most of the data are predicted to within ±20%, although a systematic tendency to under-predict $\bar{k}_r^\circ$ is apparent, especially for low conductivities. This is not surprising in view of the fact that this formula is an Ohm's law model with zero lateral conductivity, and should thus provide a lower bound to the data.

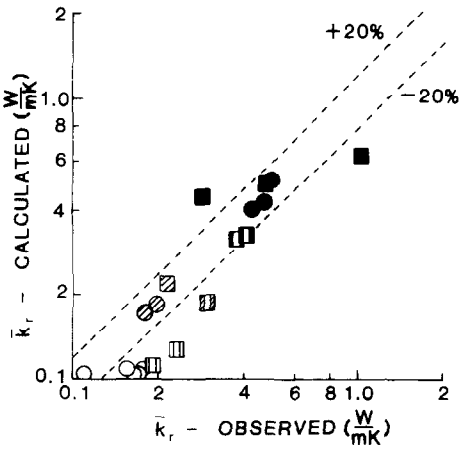

FIG. 3. Comparison of the Kunii–Smith [19] formula to bed-average conductivities.

Formula of Bauer and Schlunder [23]

This time omitting terms relevant to low pressure and surface oxide effects gives

$$\frac{k_r^\circ}{k_f} = (1-\sqrt{1-\varepsilon})+\sqrt{1-\varepsilon}\,\frac{2}{1-\frac{k_f}{k_s}B}$$

$$\times\left[\frac{\left(1-\frac{k_f}{k_s}\right)B}{\left(1-\frac{k_f}{k_s}B\right)^2}\ln\frac{k_s}{k_fB}-\frac{B+1}{2}-\frac{B-1}{1-\frac{k_f}{k_s}B}\right]$$

$$+(1-\sqrt{1-\varepsilon})\frac{k_R}{k_f}+\sqrt{1-\varepsilon}\left(\frac{k_f}{k_R}+\frac{k_f}{k_s}\right)^{-1} \qquad (12)$$

where

$$\frac{k_R}{k_f} = 2.27\times10^{-7}\left(\frac{e}{2-e}\right)T^3\frac{d_p}{k_f} \qquad (13)$$

and

$$B = C\left(\frac{1-\varepsilon}{\varepsilon}\right)^{10/9} \qquad (14)$$

with

$$C = \begin{cases} 1.25 & \text{sphere} \\ 2.5 & \text{cylinder} \\ 2.5\left[1+\left(\frac{d_i}{d_o}\right)^2\right] & \text{hollow cylinder.} \end{cases} \qquad (15)$$

Here again d_p for the radiation term is to be taken as the diameter of the equivalent-volume sphere (ignoring hollow spaces).

These equations were checked by Bauer and Schlünder [23] against data obtained by extrapolation of results from flowing fluids only, so that it might appear that equation (12) should predict bed-center values of k_r°. However the data were all for $d_t/d_p > 25$, where there would be little difference between bed-center and average values. Bauer and Schlünder [23] claim that the presence of the wall has no effect, as the decrease in conduction is offset by an increase in radiation of about the same magnitude. This will presumably depend on the temperature level of the bed, and judging from the results in Table 1 is not true here.

It was decided to compare equation (12) to both k_r° and $\bar{k}_r^\circ$, as the use of a fitting parameter C leaves some doubt as to which values it should predict. The comparison is made in Figs. 4 and 5, where it is seen that the formula overpredicts $\bar{k}_r^\circ$ and under-predicts k_r° consistently. Most of the data lie outside the $\pm 20\%$ lines, regardless of shape or conductivity. The formula is a lower-bound zero lateral conductivity Ohm's law model which employs the bed average voidage, however, the adjustment of C to extrapolation data, which are higher for low d_t/d_p than the true stagnant conductivity, confuses the issue, and is probably the reason that the formula calculations fall between the two data sets.

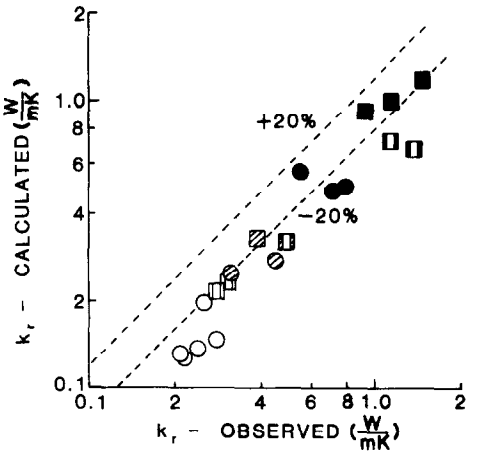

FIG. 4. Comparison of the Bauer–Schlünder [23] formula to bed-center conductivities.

The conclusions from this comparison are, that despite its limitations with regard to void fraction and lack of adjustment for different packing shapes, the Kunii–Smith formula predicts $\bar{k}_r^\circ$ reliably, with perhaps a tendency to underestimate for low conductivities, and should be used in preference to the Bauer–Schlünder model, at least for low d_t/d_p work.

APPARENT WALL-TO-SOLID HEAT TRANSFER COEFFICIENTS

Since an annular bed apparatus was used in this study, two wall Biot numbers were obtained, one for the outer wall and one for the inner wall. The outer wall Biot number Bi_b is of most interest, as it corresponds to the case of a wall-cooled catalytic reactor; inner-wall Biot numbers will be relevant to bed internal cooling tubes. It is interesting to note that Bi_a and Bi_b are not equal, as might have been inferred from [10]. In fact Bi_a

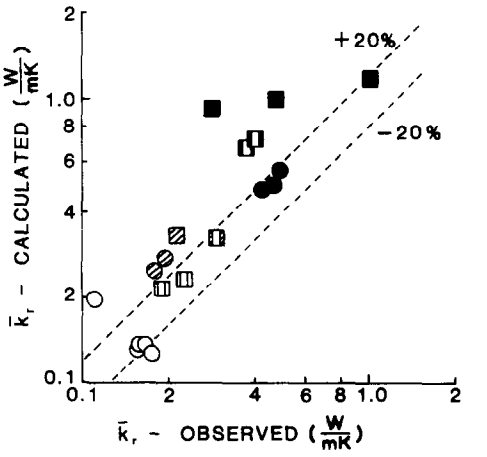

FIG. 5. Comparison of the Bauer–Schlünder [23] formula to bed-average conductivities.

is much less than Bi_b, but this difference is due to the use of different reference lengths in the definition of these quantities. There is in fact no significant difference between h_{wa} and h_{wb}, in spite of the differences in wall surface curvature between inner and outer walls. This is in agreement with the flowing fluids results of Kunii and Suzuki [34] for annular beds.

The Biot number values are plotted against d_E/d_{pv} in Figs. 6 and 7. As d_E/d_{pv} decreases, so do Bi_a and Bi_b, reflecting the decreasing number of particle-to-wall contacts per unit wall area. Most of the heat transfer takes place through the narrow gas fillets adjacent to the contact points.

There is a strong upturn in Bi_b for $d_E/d_{pv} < 4$, which is to be expected when it is recalled that

$$Bi_b = \frac{\text{bed center resistance}}{\text{extra 'near-wall' resistance}}.$$

In the limit $d_E/d_{pv} = 1$, there is only solid in the bed, so there is no extra resistance near the wall and $Bi_b = \infty$. So Bi_b must increase again as $d_E/d_{pv} \to 1$. The physical picture is that approaching low d_E/d_{pv}, the rate of loss of wall contact points slows down, while there is an increase in area contacts between surfaces of the same curvature, which eventually dominates. For Bi_a there is a similar picture, except that very thin fillets appear at low d_E/d_{pv} instead of area contacts, and the resulting upturn is not shown so strongly by the data.

The trends of the data are indicated by smoothed curves in Figs. 6 and 7. Particle conductivity has only a weak effect on both Bi_a and Bi_b, although the Bi_b for aluminum and steel packings deviate sufficiently from the curve shown to suggest that more data might justify a separate curve. Both Bi_a and Bi_b are remarkably insensitive to particle shape.

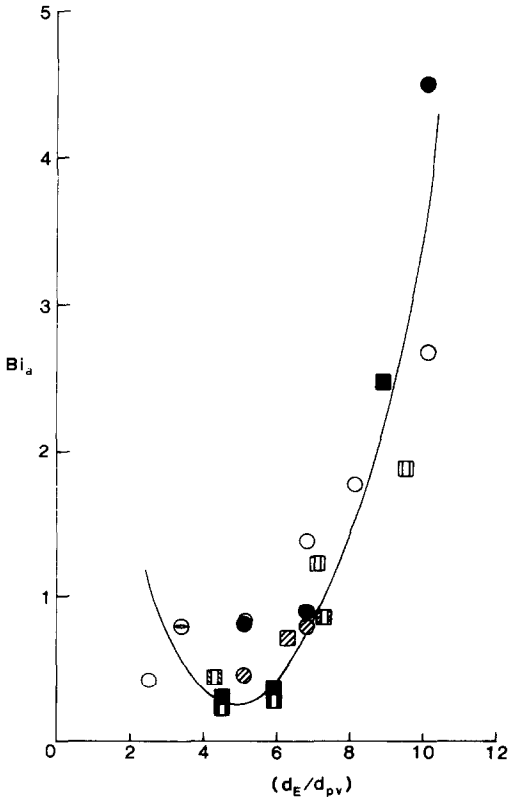

FIG. 6. Inner wall Biot number vs d_t/d_p.

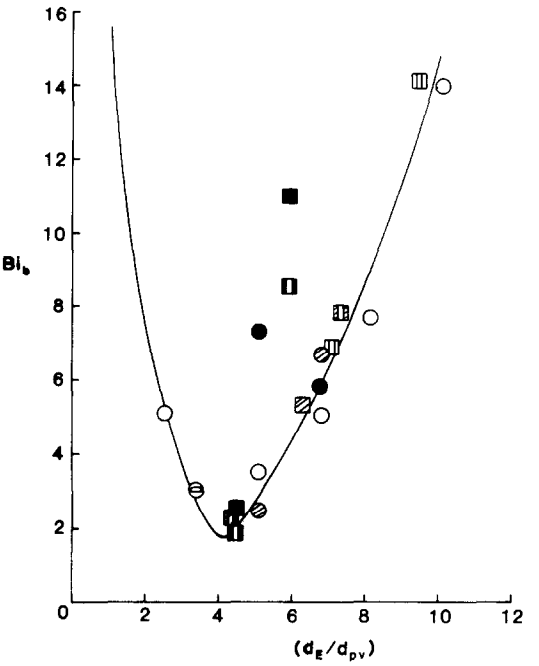

FIG. 7. Outer wall Biot number vs d_t/d_p.

The curves of Figs. 6 and 7 may be regarded as empirical correlations; for theoretical prediction few formulas are available. Olbrich [33] derived a lower bound for regular packings of spheres against a plane wall:

$$Bi_s > 2.12(R/d_p) \tag{16}$$

which is clearly not adhered to here; few details were given of the derivation of this formula, which involved several simplifications and assumptions.

The formulas of Ofuchi and Kunii [30] and Schlunder [31, 32] for h_{ws} are compared to the observed data in Table 2. That of Ofuchi and Kunii is slightly better, especially for spheres, although errors of 50% or more are common. In view of the limited work available on this parameter, and the poor agreement in Table 2, it is recommended that Bi_s is obtained from Figure 7 for low d_t/d_p.

APPLICATION TO CYLINDRICAL BEDS

The comparison of prediction formulas for k_r° and $\bar{k}_r^\circ$ made above has shown that the most accurate formula presently available is that of Kunii and Smith [19]. Their equation gives the conductivity appropriate to the void fraction used in it (i.e., bed average, bed center, near-wall etc.), and in theory could thus be used to predict either k_{rs} or $\bar{k}_{rs}$. In practice, however, it is

Table 2. Comparison of observed and predicted outer wall heat transfer coefficients

Packing	h_{wb}—observed $\left(\frac{w}{m^2 K}\right)$	h_{wb}—calculated [30] $\left(\frac{w}{m^2 K}\right)$	h_{wb}—calculated [31, 32] $\left(\frac{w}{m^2 K}\right)$
6.35 mm nylon spheres	80.97	78.45	177.31
7.938 mm nylon spheres	43.06	64.22	147.06
9.525 mm nylon spheres	33.84	55.71	126.38
12.70 mm nylon spheres	26.11	43.76	99.76
25.40 mm nylon spheres	34.00	24.69	57.61
6.35 mm steel spheres	∞	154.57	172.44
9.525 mm steel spheres	138.93	110.01	120.85
12.70 mm steel spheres	111.36	84.65	93.91
6.35 × 6.35 mm Al cylinders	∞	154.58	154.19
9.525 × 9.525 mm Al cylinders	394.75	112.30	107.59
12.70 × 12.70 mm Al cylinders	68.37	88.28	83.42
9.525 × 9.525 × 4.673 mm Al hollow cylinders	271.15	123.57	107.59
12.70 × 12.70 × 6.35 mm Al hollow cylinders	67.69	87.91	83.42
6 × 6 × 4 mm glass hollow cylinders	119.46	81.70	167.48
8 × 8 × 6 mm glass hollow cylinders	52.35	40.94	132.05
9.525 mm porous ceramic spheres	54.89	79.20	127.48
12.70 mm porous ceramic spheres	29.68	60.53	100.87
9.525 × 9.525 mm porous ceramic cylinders	52.31	65.02	114.17
7.94 × 7.94 × 3.97 mm porous ceramic hol. cyl.	101.76	80.38	132.48

unlikely that anything more than the average voidage would be easily measurable, and thus only $\bar{k}_{rs}$ could be readily obtained.

The bed center k_{rs}, however, appears to be necessary for the use of a two-phase model or any consequences of the use of that model. In particular, a model-matching formula for the effective radial Peclet number for fixed-bed heat transfer has been derived as [3]:

$$\frac{1}{Pe_r} = \frac{1}{Pe_{rf}} + \frac{k_{rs}}{k_f}(Re\,Pr)^{-1}\left(\frac{Bi_f+4}{Bi_f}\right) \times \left[\frac{8}{N_s} + \frac{Bi_s+4}{Bi_s}\right]^{-1} \quad (17)$$

where

$$N_s = \frac{1.5(1-\varepsilon)(d_t/d_p)^2}{\frac{k_{rs}}{k_f}\left\{\frac{1}{Nu_{fs}} + \frac{0.1}{k_p/k_f}\right\}} \quad (18)$$

and clearly requires knowledge of k_{rs}.

The most convenient method of obtaining k_{rs} is to predict $\bar{k}_{rs}$ and then use a relation between the two quantities to correct $\bar{k}_{rs}$ for wall effects. This cannot be done empirically from annular bed data, as for that case $\bar{k}_{rs}$ contains resistances at both walls, whereas for cylindrical beds a predicted $\bar{k}_{rs}$ would include only a single wall resistance, that of the outer wall.

The relationship between the overall heat transfer coefficient U and the effective parameters k_r and h_w is well known [35] for one- and two-dimensional pseudohomogeneous continuum models. It may be extended to show that using a similar relation for the solid phase of a two-phase continuum model can give

$$\frac{k_{rs}}{\bar{k}_{rs}} = 1 + \frac{4}{Bi_s} = \frac{Bi_s+4}{Bi_s} \quad (19)$$

in dimensionless form. This formula predicts much less of an increase in k_{rs} over $\bar{k}_{rs}$ for the cylindrical bed for which it was derived, than the empirical formula of Wellauer *et al* [4], which was based on annular bed

data, and therefore corrected for the inclusion of both inner and outer near-wall resistances.

The similarity of the solid-phase Biot number group in equation (19) to that in equation (17) prompts closer examination of the latter. The quantity N_s increases with Re, as Nu_{fs} does, and for $Re > 100$ approximately,

$$\frac{8}{N_s} \ll \frac{Bi_s+4}{Bi_s}. \tag{20}$$

Thus neglecting the interphase transport term $8/N_s$ gives

$$\frac{1}{Pe_r} = \frac{1}{Pe_{rf}} + \frac{k_{rs}}{k_f}(Re\,Pr)^{-1}\left(\frac{Bi_f+4}{Bi_f}\right)\left(\frac{Bi_s}{Bi_s+4}\right) \tag{21}$$

and associating solid-phase terms allows this formula to be rewritten using equation (19) as

$$\frac{1}{Pe_r} = \frac{1}{Pe_{rf}} + \frac{\bar{k}_{rs}}{k_f}(Re\,Pr)^{-1}\left(\frac{Bi_f+4}{Bi_f}\right) \tag{22}$$

which will be referred to hereafter as the *short form* of equation (17).

The difference between the short form and the full form of equation (17) is very slight, as shown in Fig. 8, where the experimental data of Dixon *et al.* [2] are included for comparison. This reflects the relative unimportance of interphase transport in steady-state heat transfer models without reaction. The lines shown were computed for $d_t/d_p = 7.5$ and $Pe_{rf} = 10.0$, and Bi_f was given by an empirical formula derived from mass transfer studies [5].

It should be noted that if it is incorrectly assumed that $Bi_s = \infty$, and a bed average conductivity used in equation (17) in place of the required bed center one, a formula is obtained which differs from the short form only by the interphase term, and is thus in good agreement with it.

$$\frac{1}{Pe_r} = \frac{1}{Pe_{rf}} + \frac{\bar{k}_{rs}}{k_f}(Re\,Pr)^{-1}\left(\frac{Bi_f+4}{Bi_f}\right)\left(1+\frac{8}{N_s}\right). \tag{23}$$

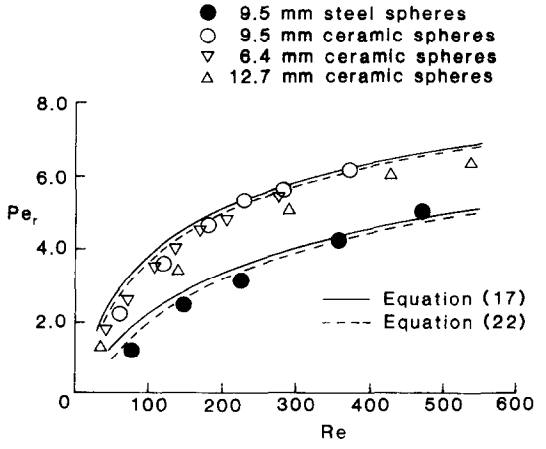

FIG. 8. Comparison of equation (17) with equation (22) and with effective radial Peclet number data.

This, in fact, was the approach used previously [3] and it is now clear that the good agreement with data in that work was somewhat fortuitous, in that two compensating incorrect assumptions ($Bi_s = \infty$ and $k_{rs} = \bar{k}_{rs}$) were made, which would only cause difficulties in this lumping technique if interphase transfer were important.

Simulations using a two-phase model, on the other hand, showed the need for a finite Bi_s [36] for good agreement between fluid-phase and measured temperature profiles. In that work, the bed average conductivity $\bar{k}_{rs}$ was used, for want of any better estimate, instead of k_{rs}. It was necessary to lower Pe_{rf} (i.e. increase k_{rf}) to improve the simulations, but no justification could be found for that step. The need for higher k_{rf} is here revealed as compensating for an underestimated k_{rs}.

For future prediction of Pe_r it is here recommended that the short form, equation (22), be used, as this dispenses with the correlation for Nu_{fs}, and also allows the direct use of $\bar{k}_{rs}$, which can be predicted from the Kunii–Smith formula using average bed voidage.

CONCLUSIONS

The Kunii–Smith formula (equation (6)) unambiguously predicts $\bar{k}_r^\circ$ from the bed average void fraction, which is usually the only voidage measurement available. The formula is good to $\pm 20\%$ for a wide range of conductivities and pellet shapes, and is to be preferred for low d_t/d_p beds. The bed center k_r° may be obtained by subtracting out the wall effects using equation (19).

For low d_t/d_p beds the solid-phase resistance to heat transfer near the wall is quite substantial. Predictive formulas are rather inaccurate, and the wall-to-wall Biot number should be obtained from Fig. 7 for reasonably low-conductivity packings.

The effective radial conductivity k_r may be related to the single-phase parameters by a somewhat simpler equation than previously suggested. The role of the solid-phase terms is now clarified, and slightly contradictory findings from two earlier studies are thereby reconciled.

Acknowledgements—The authors would like to thank Norton Company, Chemical Process Products Division, for donating the porous ceramic packings, and Worcester Polytechnic Institute for support provided to one of the authors (MMM) during this work.

REFERENCES

1. J. B. Agnew and O. E. Potter, Heat transfer properties of packed tubes of small diameter, *Trans. Instn. Chem. Engrs.* **48**, T15-T20 (1970).
2. A. G. Dixon, D. L. Cresswell and W. R. Paterson, Heat transfer in packed beds of low tube/particle diameter-ratio, *Chemical Reaction Engineering—Houston* (edited by V. W. Weekman and D. Luss), ACS Symp. Ser. No. 65, 238–253 (1978).
3. A. G. Dixon and D. L. Cresswell, Theoretical prediction of

effective heat transfer parameters in packed beds, *AIChE J.* **25,** 663–676 (1979).
4. T. Wellauer, D. L. Cresswell and E. J. Newson, Heat transfer in packed reactor tubes suitable for selective oxidation, *Chemical Reaction Engineering—Boston* (edited by J. Wei and C. Georgakis), ACS Symp. Ser. No. 196, 527–542 (1982).
5. A. G. Dixon, M. A. DiCostanzo and B. A. Soucy, Fluid-phase radial transport in packed beds of low tube-to-particle diameter ratio, *Int. J. Heat Mass Transfer* **27,** 1701–1713 (1984).
6. A. L. Waddams, The flow of heat through granular material, *J. Soc. Chem. Ind.* **63,** 337–340 (1944).
7. R. A. Sehr, The thermal conductivity of catalyst particles, *Chem. Engng Sci.* **9,** 145–152 (1958).
8. S. Yagi and D. Kunii, Studies on heat transfer near wall surface in packed beds, *AIChE J.* **6,** 97–104 (1960).
9. T. Koya and D. Kunii, Measurement of thermal conductivities of solid particles in packed beds, *Int. Chem. Engng* **12,** 162–167 (1972).
10. W. R. Paterson, Some aspects of the mathematical modelling of fixed bed chemical reactors, Ph.D. Thesis, Univ. of Edinburgh (1975).
11. R. A. Crane and R. I. Vachon, A prediction of the bounds on the effective thermal conductivity of granular materials, *Int. J. Heat Mass Transfer* **20,** 711–723 (1977).
12. N. Wakao and K. Kato, Effective thermal conductivity of packed beds, *J. Chem. Engng Japan* **2,** 24–38 (1969).
13. P. W. Dietz, Effective thermal conductivity of packed beds, *Ind. Engng Chem. Fund.* **18,** 283–286 (1979).
14. A. R. Balakrishnan and D. C. T. Pei, Heat transfer in gas–solid packed bed systems, 2. The conduction mode, *Ind. Engng Chem. Proc. Des. Dev.* **18,** 40–46 (1979).
15. R. C. McPhedran and D. R. McKenzie, The conductivity of lattices of spheres, I. The simple cubic lattice, *Proc. R. Soc. Lond.* **A359,** 45–62 (1978).
16. A. S. Sangani and A. Acrivos, On the effective thermal conductivity and permeability of regular arrays of spheres, *Lecture Notes in Physics* **154,** 216–225, Springer-Verlag, Berlin (1982).
17. H.-C. Chang, Effective diffusion and conduction in two-phase media: a unified approach, *AIChE J.* **29,** 846–853 (1983).
18. S. Yagi and D. Kunii, Studies on effective thermal conductivities in packed beds, *AICHE J.* **3,** 373–381 (1957).
19. D. Kunii and J. M. Smith, Heat transfer characteristics of porous rocks, *AIChE J.* **6,** 71–78 (1960).
20. G. P. Willhite, D. Kunii and J. M. Smith, Heat transfer in beds of fine particles (heat transfer perpendicular to flow), *AIChE J.* **8,** 340–345 (1962).
21. V. Specchia, G. Baldi and S. Sicardi, Heat transfer in packed bed reactors with one phase flow, *Chem. Eng. Commun.* **4,** 361–380 (1980).
22. P. Zehner and E. U. Schlünder, Wärmeleitfähigkeit von Schüttungen bei maßigen Temperaturen, *Chemie-Ingr.-Techn.* **42,** 933–941 (1970).
23. R. Bauer and E. U. Schlünder, Effective radial thermal conductivity of packings in gas flow. Part II Thermal conductivity of the packing fraction without gas flow, *Int. Chem. Engng* **18,** 189–204 (1978).
24. P. Zehner and E. U. Schlünder, Einfluß der Wärmestrahlung und des Druckes auf den Wärmetransport in nicht durchströmten Schüttungen, *Chemie-Ingr.-Techn.* **44,** 1303–1308 (1972).
25. J. C. Chen and S. W. Churchill, Radiant heat transfer in packed beds, *AIChE J.* **9,** 35–41 (1963).
26. Y. C. Chiew and E. D. Glandt, Simultaneous conduction and radiation in porous and composite materials: effective thermal conductivity, *Ind. Engng Chem. Fund.* **22,** 276–282 (1983).
27. C. K. Chan and C. L. Tien, Conductance of packed spheres in vacuum, *J. Heat Transfer* **95,** 302–208 (1973).
28. N. Wakao and D. Vortmeyer, Pressure dependency of effective thermal conductivity of packed beds, *Chem. Engng Sci.* **26,** 1753–1765 (1971).
29. R. Krupiczka, Analysis of thermal conductivity in granular materials, *Int. Chem. Engng* **7,** 122–144 (1967).
30. K. Ofuchi and D. Kunii, Heat transfer characteristics of packed beds with stagnant fluids, *Int. J. Heat Mass Transfer* **8,** 749–757 (1965).
31. E. U. Schlünder, Wärmeübergang an bewegte Kugelschüttungen bei kurzfristigem Kontakt, *Chemie-Ingr-Techn.* **43,** 651–654 (1971).
32. E. U. Schlünder, Transport phenomena in packed bed reactors, *Chemical Reaction Engineering Reviews—Houston* (edited by D. Luss and V. W. Weekman), ACS Symp. Ser. No. 72, 110–161 (1978).
33. W. E. Olbrich, A two-phase diffusional model to describe heat transfer processes in a non-adiabatic packed tubular bed, *Instn. Chem. Engrs Symp. Ser.* **33,** 101–119 (1971).
34. D. Kunii and M. Suzuki, Heat transfer between wall surface and packed solids, *Int. Heat Transfer Conf. (Chicago)* IV, 344–352 (1966).
35. G. F. Froment, Fixed bed reactors. Steady-state conditions, *Proc. 2nd ISCRE*, Amsterdam pA5-1-A5-20, Elsevier (1972).
36. A. G. Dixon, Solution of packed-bed heat-exchanger models by orthogonal collocation using piecewise cubic Hermite functions, *Chemical Reactors* (edited by H. S. Fogler), ACS Symp. Ser. No. 168, 287–304 (1981).

CONDUCTION DANS LE SOLIDE A L'INTERIEUR DE LITS DE SPHERES, DE BOULETS ET D'ANNEAUX A FAIBLE d_t/d_p

Résumé—Des mesures expérimentales de conductivité thermique effective et de coefficients de transfert thermique à la paroi sont faites pour des lits fixes annulaires avec un faible rapport de diamètres tube-particule. Elles couvrent un large domaine de forme de particule, de taille et de conductivité thermique. Des formules empiriques sont données pour le coefficient de transfert thermique pariétal qui devient important pour d_t/d_p faible. Des formules prédictives pour la conductivité thermique sont testées et on fait des recommendations sur leur utilisation. Des paramètres sont trouvés relativement insensibles à la forme de la particule. Les résultats sont appliqués à l'estimation de la conductivité effective dans les lits cylindriques d'intérêt industriel.

FESTKÖRPER-WÄRMELEITUNG IN BETTEN AUS KUGELN, PELLETS UND RINGEN

Zusammenfassung—Die effektive Wärmeleitfähigkeit und der Wärmeübergangskoeffizient an der Wand von ruhenden Festbetten mit kreisringförmigem Querschnitt und kleinem Verhältnis Rohr-/Partikeldurchmesser (d_t/d_p) wurden experimentell untersucht. Dabei wurde ein weiter Bereich von Formen, Größen und Wärmeleitfähigkeiten der Partikel abgedeckt. Für den Wärmeübergangskoeffizienten zwischen Wand und Festkörper, der besonders wichtig für kleine d_t/d_p ist, wurden empirische Korrelationen angegeben. Berechnungsgleichungen für die Wärmeleitfähigkeit wurden überprüft und beurteilt. Beide Parameter erwiesen sich als weitgehend unabhängig von der Form der Partikel. Die Ergebnisse werden dazu verwendet, die effektive Wärmeleitfähigkeit von zylindrischen Betten der industriellen Praxis zu berechnen.

ТЕПЛОПРОВОДНОСТЬ СФЕР, ГРАНУЛ И КОЛЕЦ В СЛОЯХ С МАЛЫМ d_t/d_p

Аннотация—Экспериментально измерены коэффициенты эффективной теплопроводности и теплопереноса к стенке в неподвижных кольцевых слоях с малым отношением диаметра трубы к диаметру частиц. Исследования проводились в широком диапазоне изменения форм, размеров и теплопроводностей частиц. Приведены эмпирические зависимости для определения коэффициентов теплопереноса между стенкой и твердыми частицами, которые играют существенную роль при малом отношении d_t/d_p. Проверены теоретические формулы для расчета теплопроводности и даны рекомендации по их использованию. Обнаружено, что форма частиц не оказывает существенного влияния на оба исследуемых параметра. Полученные результаты использованы для оценки эффективной теплопроводности в цилиндрических слоях промышленного масштаба.